J Mater Sci (2011) 46:4937–4941
DOI 10.1007/s10853-011-5406-y

Thermo-mechanical properties of $La_2NiO_{4+\delta}$

B. X. Huang · J. Malzbender · R. W. Steinbrech

Received: 16 December 2010 / Accepted: 15 February 2011 / Published online: 24 February 2011

Abstract Elastic and fracture behavior of $La_2NiO_{4+\delta}$ have been assessed. Fracture stress and elastic modulus of porous $La_2NiO_{4+\delta}$ were evaluated from room temperature (RT) up to 900 °C on the basis of 4-point bending tests. Both parameters increase slightly from RT to 700 °C. However, at higher temperatures the elastic modulus decreases, whereas the fracture stress increases. In addition, elastic modulus and damping/internal friction of dense specimens were measured by a resonance method. A strong change of elastic modulus and internal friction between RT and 100 °C appears to be related to an orthorhombic-tetragonal phase transition. No indications of phase transition can be observed at higher temperatures. Although thermogravimetric measurements suggest that oxygen was continuously released from the lattice up to 1000 °C with increasing temperature, the thermal expansion coefficient showed a rather stable value from RT up to 1000 °C.

Introduction

Mixed ionic and electronic conductors are promising materials for the application as cathodes of solid oxide fuel cell and ceramic membranes for oxygen separation [1–9]. One material under consideration as membrane, $La_2NiO_{4+\delta}$ possesses a K_2NiF_4 crystal structure, which can be described as alternating perovskite and rock salt layers along the c-direction [3, 10] (Fig. 1). $La_2NiO_{4+\delta}$ phases are oxygen-hyperstoichiometric ($\delta > 0$) below $\sim$1000 °C with an oxygen non-stoichiometry close to 0.14 at RT when slowly cooled in air [13–17]. The oxygen ion transport in $La_2NiO_{4+\delta}$ occurs via a complex mechanism combining interstitial migration in the rock salt layers and vacancy migration in the perovskite layers [11, 12].

The apparent advantages of $La_2NiO_{4+\delta}$ oxygen transport membranes include high chemical stability, stable thermal expansion, and low chemical expansion compared to perovskite type materials. The isothermal chemical expansion caused by a change of oxygen partial pressure is less than 0.05% [3, 18], which reduces thermo-mechanical stability problems during operation.

Mechanical integrity is an important issue for practical membrane application. Typically stresses can be induced by thermal and chemical gradients as well as differences in thermal expansion compared to sealing and housing materials. In fact permeation can be increased by reducing the membrane thickness, which leads to the necessity to deposit the membrane on a porous substrate material. In order to avoid stresses due to differences in thermal expansion coefficient membrane material and substrate should be identical. Hence the mechanical properties of the substrate materials will be crucial for the mechanical reliability of the entire assembly and are in addition necessary for the analysis and modeling of deformation and stress state of the composite. Hence the mechanical properties of porous $La_2NiO_{4+\delta}$ have been characterized. Additional experiments have been carried out to assess the elastic behavior of dense material that appear to be representative for membrane layers that can be deposited on the porous substrate.

Information on the thermo-mechanical properties of $La_2NiO_{4+\delta}$ is limited. In this study, elastic and fracture properties of porous $La_2NiO_{4+\delta}$ have been determined as a function of temperature as obtained using 4-point bending tests and for dense material using a non-destructive resonance vibration based method. In general, porous material

B. X. Huang · J. Malzbender (✉) · R. W. Steinbrech
Forschungszentrum Jülich GmbH, Institute of Energy and Climate Research 2 (IEK-2), 52425 Jülich, Germany
e-mail: j.malzbender@fz-juelich.de

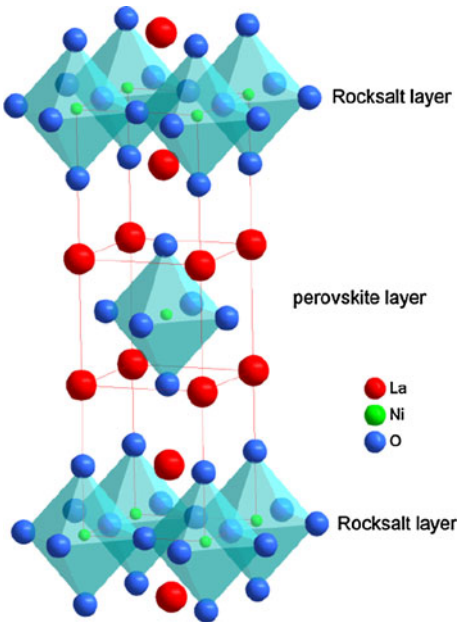

Fig. 1 Atomic structure of $La_2NiO_{4+\delta}$

has a strong vibrational damping. Hence the resonance method could not be use for porous $La_2NiO_{4+\delta}$. The linear thermal expansion was measured using a dilatometer.

Experiments

Samples prepared from spray pyrolysis powders were sintered at 1400 °C in air with a cellulose-based pore former to obtain a membrane material with a defined pore structure (porosity ~ 52%) (Fig. 2). The specimens were extruded and possessed a rectangular shape of 50 × 8.4 × 5.7 mm^3, which are the conditions in real application. In addition, dense bars (porosity ~ 6%) with a dimension

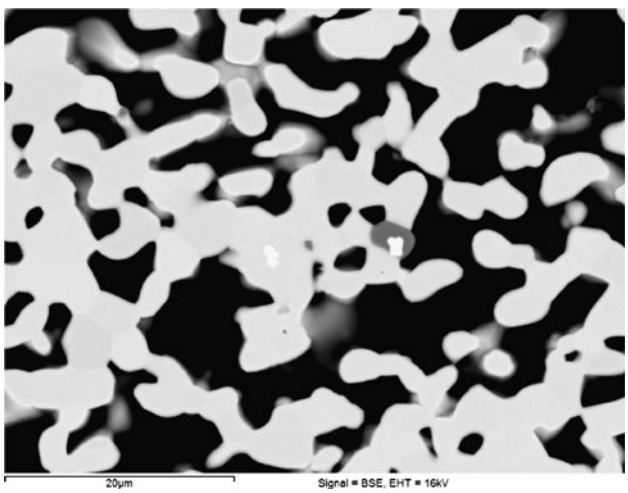

Fig. 2 Porous structure of $La_2NiO_{4+\delta}$ specimens

of 4 × 2.8 × 32 mm^3 were prepared by the IEK-1 (Forschungszentrum Jülich GmbH) by sintering at 1400 °C in air for 3 h.

The elastic modulus and fracture stress of the porous samples were determined from 4-point bending tests [19] with a universal mechanical testing machine (Instron 1362). The tests were carried out at selected temperatures in the range RT to 900 °C. For tests at elevated temperatures, a heating rate of 4 K/min was chosen with a subsequent dwell time of 1 h before testing to reach thermal equilibrium. In all tests, the load rate was 50 N/min and five samples were tested for each temperature. The elastic modulus was determined from the loading–displacement curve.

Furthermore, the elastic modulus and internal friction (Q^{-1}) of the dense materials were determined from the resonance frequency of the bar-shaped specimens in the temperature range RT–950 °C in air. An impulse excitation method (Grindosonic, Lemmens KG, Belgium) was used with a heating rate of 1 K/min. The resonant behavior of the unconstrained specimens was analyzed with an in-house data acquisition program, which permitted an additional assessment of the decay of the resonance frequency (damping behavior). The elastic modulus was determined as outlined in ASTM E1876-09. The internal friction Q^{-1} is defined as [20]:

$$Q^{-1} = (1/n)\ \ln(A_0/A_n) \tag{1}$$

where n is the number of the vibration cycles, while its amplitude attenuates from A_0 to A_n.

The linear thermal expansion coefficient (TEC) was measured by using a differential dilatometer (Misura, Expert System Solutions S.r.l. Italia) in the temperature range from RT up to 1000 °C. The heating rate in these measurements was 1 K/min. The effective technical thermal expansion coefficient α was calculated using

$$\alpha = \frac{1}{L0}\frac{L - L0}{T - T0} \tag{2}$$

where L is the specimen length measured at a given temperature T, while L_0 corresponds to the initial length of the specimen at RT (T_0). Differential thermal analysis (DTA) and thermogravimetry (TG) (STA 449C Jupiter Netzsch) were carried out in air with a heating rate of 3 K/min.

Results and discussion

The temperature dependence of the average elastic modulus of the porous $La_2NiO_{4+\delta}$ as obtained from 4-point bending test data is given in Fig. 3. The values appear to increase slightly from RT to 800 °C. However, considering the scatter of the data, it can be stated that the elastic

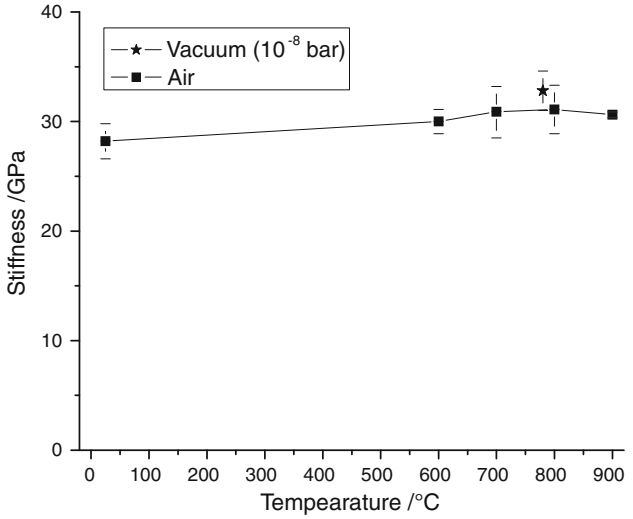

Fig. 3 Elastic modulus of the porous specimens as a function of temperature and atmosphere

modulus of the porous material is independent of the temperature within the limits of uncertainty. Note that the values appear to be slightly higher under vacuum (10^{-8} bar) than in air at 800 °C. The results correlate with the reported higher oxygen deficiency under vacuum at a particular temperature [21, 22].

An assessment of the elastic properties with the resonance method was not possible for porous samples. Hence, dense bars of $La_2NiO_{4+\delta}$ were sintered for the dynamic measurement of elasticity. Corresponding results for elastic modulus and the internal friction are shown in Fig. 4. In particular, the internal friction has been proved to be a sensitive and nondestructive methodology to assess phase transitions in solids [23–25]. The modulus decreases from RT to 100 °C by ~10%, and further decreases slightly with increasing temperature up to 950 °C similar as reported for most ceramic materials [26]. The internal friction exhibits higher values between RT and 100 °C, and then remains relatively stable up to 950 °C. As expected, the elastic moduli obtained for the porous material are significantly lower than the values for the dense specimens. Note that the small temperature dependency observed for the dense bars could not be obtained for the porous material due to the rather large uncertainty in the mechanical tests.

The maximum in the internal friction data at ~90 °C agrees very well with the orthorhombic-tetragonal transition reported by Brill et al. [27]. Also Skinner [28] stated that an orthorhombic-tetragonal transition occurs between RT and 150 °C, and that the tetragonal structure is maintained from 150 to 800 °C. The strong change of elastic modulus measured in the same temperature range appears to reflect this phase transition. Above this temperature, no indication for further phase transitions could be observed in the internal friction curve.

The average fracture stresses of the porous material obtained in 4-point bending increase slightly from RT to 700 °C, but again this effect is within the limits of experimental uncertainty. However, a strong increase is observed from 700 to 900 °C (Fig. 5). Since the measurements were carried out with as-received samples, internal stresses in the sample may be generated by fast cooling and limitations in oxygen diffusion. Thus, the increase of fracture stress with temperature might be associated with a relaxation of residual stresses. To exclude the influence of such effects, samples were also annealed at 800 °C for 2 h with a heating rate of 4 K/min and a cooling rate of 0.1 K/min. In fact the fracture stress of the annealed samples is ~25% higher than that of as-received samples, and is equal to the fracture stress of samples tested at 600 and 700 °C. Therefore, the increase of fracture stress from RT to 700 °C can be

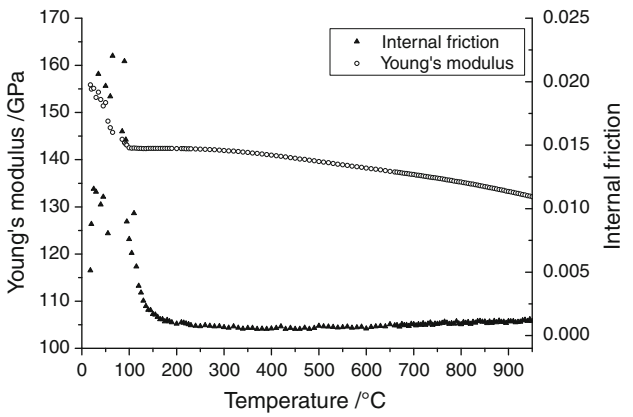

Fig. 4 Elastic modulus and internal friction of dense $La_2NiO_{4+\delta}$ as a function of temperature

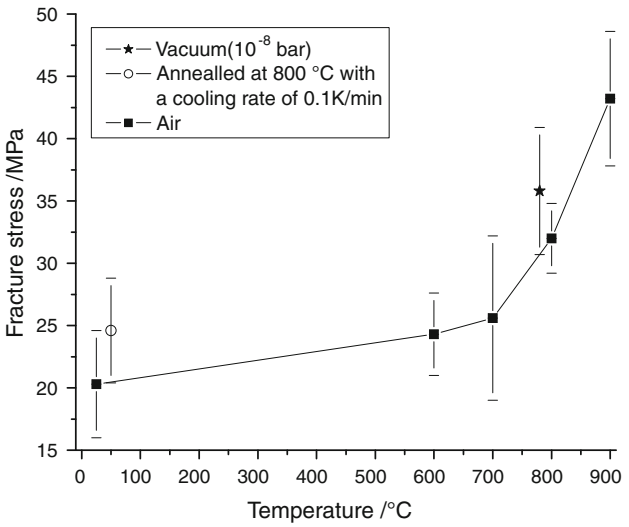

Fig. 5 Fracture stress of the porous $La_2NiO_{4+\delta}$ as a function of temperature and atmosphere

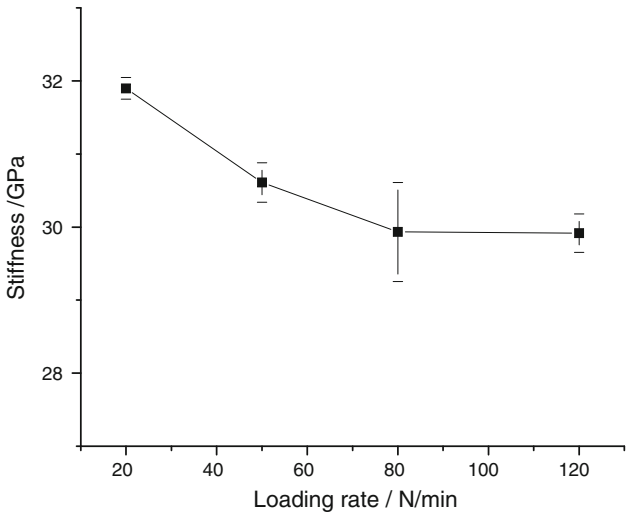

Fig. 6 Dependence of the stiffness of porous $La_2NiO_{4+\delta}$ on loading rate at 900 °C

attributed to the elimination of residual stresses. Since no phase transition was observed between 700 and 900 °C, the increase of the fracture stress might be related to creep in the highly stressed areas.

In order to investigate the assumed creep effects, the stiffness of a porous sample was measured at 900 °C applying loading rates between 120 and 20 N/min (Fig. 6). Without creep no influence of the loading rate should be observed, otherwise a decrease with decreasing loading rate can be expected. However, an opposite result was obtained from the experiments. The elastic modulus increased with decreasing loading rate. Since the sample was measured in a sequence from high to low loading rate, it proves that the creep is initially very high (primary creep), but slows down quickly with increasing strain. Therefore, although the steady state creep could be very low between 800 and 900 °C, the primary creep could have contributed to the stress relaxation.

The stoichiometry of oxygen was measured with TG, assuming that only oxygen is released during heating. The initial oxygen stoichiometry is supposed to be 4.14 [13, 14, 16, 17]. The stoichiometry and DTA curves are shown in Fig. 7. The sample starts to lose oxygen from ~400 °C, and the δ decreases continuously from this temperature up to 1000 °C. No effect can be observed in the DTA curve.

The thermal expansion coefficient keeps stable up to 1000 °C (Fig. 8). The value of TEC is in good agreement with earlier reports [3, 28]. No obvious indications of chemical expansion could be observed. Normally, the thermal expansion is due to the anharmonic vibration of the lattice, which increases slightly with temperature [29], as observed for Al_2O_3 and stainless steel. For comparison, the TEC values of Al_2O_3, stainless steel and $Ba_{0.5}Sr_{0.5}Co_{0.8}Fe_{0.2}O_{3-\delta}$ (BSCF) are also given. BSCF is another candidate

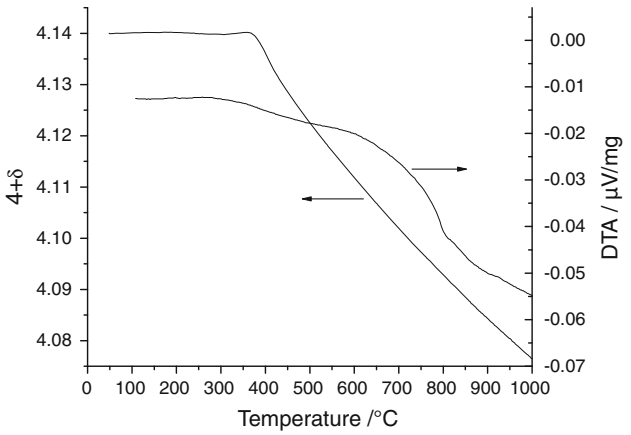

Fig. 7 Oxygen stoichiometry and DTA of porous samples

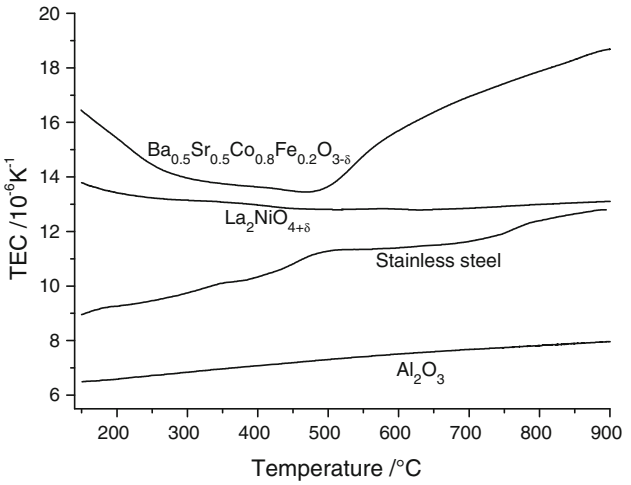

Fig. 8 Thermal expansion of porous $La_2NiO_{4+\delta}$. For comparison, thermal expansion curves of $Ba_{0.5}Sr_{0.5}Co_{0.8}Fe_{0.2}O_3$, Al_2O_3, and stainless steel are also given

material for oxygen transport membranes. The high TEC values of BSCF at low temperature are due to spin transition of Co^{3+} [30], and at high temperature the influence of chemical expansion causes the rise. The high TEC values of $La_2NiO_{4+\delta}$ at low temperatures might be related with the orthorhombic structure. $La_2NiO_{4+\delta}$ phases are oxygen-hyperstoichiometric ($\delta > 0$), and the oxygen stoichiometry is about 4.08 at 1000 °C (Fig. 7). Hence, interstitial oxygen is lost only partly during heating. Unlike lattice oxygen, interstitial oxygen should not lead to significant chemical expansion.

Conclusion

A strong change of elastic modulus and internal friction observed for dense specimens between RT and 100 °C

might be attributed to an orthorhombic-tetragonal transition. No indication of phase transition could be observed from 150 °C up to 950 °C. The fracture properties of porous $La_2NiO_{4+\delta}$ samples were measured with 4-point bending tests. The increase of fracture stress from 700 to 900 °C is attributed to the primary creep. Oxygen was continuously released from ~400 °C up to 1000 °C with increasing temperature. The thermal expansion coefficient keeps almost a stable value from RT up to 1000 °C.

Acknowledgements The study was funded by the German Ministry of Economics and Technology as part of the research activities in the project OXYMEM (code: 0327739B). The authors wish to thank Dr. Baumann for the preparation of the dense specimens, and Dr. Möbius for TG/DTA measurements.

References

1. Aguadero A, Alonso JA, Martinez-Lope MJ, Fernandez-Diaz MT, Escudero MJ, Daza L (2006) J Mater Chem 16:3402
2. Bassat JM, Odier P, Villesuzanne A, Marin C, Pouchard M (2004) Solid State Ion 167:341
3. Tsipis EV, Naumovich EN, Shaula AL, Patrakeev MV, Waerenborgh JC, Kharton VV (2008) Solid State Ion 179:57
4. McIntosh S, Vente JF, Haije WG, Blank DHA, Bouwmeester HJM (2006) Solid State Ion 177:1737
5. Vente JF, Haije WG, Rak ZS (2006) J Membr Sci 276:178
6. Shao ZP, Yang WS, Cong Y, Dong H, Tong JH, Xiong GX (2000) J Membr Sci 172:177
7. Liu LM, Lee TH, Qiu L, Yang YL, Jacobson AJ (1996) Mater Res Bull 31:29
8. Tai LW, Nasrallah MM, Anderson HU, Sparlin DM, Sehlin SR (1995) Solid State Ion 76:259
9. Sunarso J, Baumann S, Serra JM, Meulenberg WA, Liu S, Lin YS, da Costa JCD (2008) J Membr Sci 320:13
10. Naumovich EN, Patrakeev MV, Kharton VV, Yaremchenko AA, Logvinovich DI, Marques FMB (2005) Solid State Sci 7:1353
11. Kharton VV, Yaremchenko AA, Naumovich EN (1999) J Solid State Electrochem 3:303
12. Minervini L, Grimes RW, Kilner JA, Sickafus KE (2000) J Mater Chem 10:2349
13. Rice DE, Buttrey DJ (1993) J Solid State Chem 105:197
14. Kanai H, Mizusaki J, Tagawa H, Hoshiyama S, Hirano K, Fujita K, Tezuka M, Hashimoto T (1997) J Solid State Chem 131:150
15. Vashook VV, Tolochko SP, Yushkevich L, Makhnach LV, Kononyuk IF, Altenburg H, Hauck J, Ullmann H (1998) Solid State Ion 110:245
16. Vashook VV, Yushkevich II, Kokhanovsky LV, Makhnach LV, Tolochko SP, Kononyuk IF, Ullmann H, Altenburg H (1999) Solid State Ion 119:23
17. Tamura H, Hayashi A, Ueda Y (1993) Physica C 216:83
18. Kharton VV, Kovalevsky AV, Avdeev M, Tsipis EV, Patrakeev MV, Yaremchenko AA, Naumovich EN, Frade JR (2007) Chem Mater 19:2027
19. Zhu AH, Christofides PD, Cohen Y (2010) J Membr Sci 346:361
20. Du J, Sun Y, Jiang J, Zeng F, Yin H (1990) Phys Rev B 41:6679
21. Mantzavinos D, Hartley A, Metcalfe IS, Sahibzada M (2000) Solid State Ion 134:103
22. Nakamura T, Petzow G, Gauckler LJ (1979) Mater Res Bull 14:649
23. Zhang HL, Wu XS, Chen CS, Liu W (2005) Phys Rev B 71:064422
24. Zheng RK, Huang RX, Tang AN, Li G, Li XG, Wei JN, Shui JP, Yao Z (2002) Appl Phys Lett 81:3834
25. Zheng RK, Tang AN, Yang Y, Wang W, Li G, Li XG, Ku HC (2003) J Appl Phys 94:514
26. Watchman JB (1996) Mechanical properties of ceramics. Wiley, New York
27. Brill TM, Hampel G, Mertens F, Schurmann R, Assmus W, Luthi B (1991) Phys Rev B 43:10548
28. Skinner SJ (2003) Solid State Sci 5:419
29. Barsoum MW (2003) Fundamentals of ceramics. Institute Of Physics Publishing (Gb), London
30. Huang BX, Malzbender J, Steinbrech RW, Grychtol P, Schneider CM, Singheiser L (2009) Appl Phys Lett 95:051901